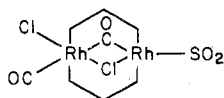


electrolyte. The above data are consistent with terminal attack of SO_2 and the formation of an intermediate species of the form



This species is then believed to lose Cl^- and to rearrange to the final product **3b**, having a bridging SO_2 ligand. We have obtained similar results when CS_2 instead of SO_2 is used.³⁴ In this case the chemistry parallels that which we propose for the SO_2 complex except that the intermediate species have longer lifetimes (days) so detailed spectroscopic measurements can be (and have been) made supporting our proposed scheme for the SO_2 reaction.

(e) Site of SO_2 Attack in $[\text{Rh}_2(\text{CO})_2(\mu\text{-Cl})(\text{DPM})_2]^+$. In these "A-frame" species there are two potential sites of attack, either directly at the enclosed site, bridging the metal centers, or at a terminal, exposed position remote from the bridging site. It has been shown that CO attacks **1a** terminally, forcing one of the previously coordinated carbonyl ligands into the bridge.^{2,4} Likewise CO appears to attack the SO_2 "A-frame" complex **4** terminally since again no evidence was obtained for attack at the bridging site. In contrast, SO_2 appears to attack complex **1** directly at the bridging site, which has been shown to be open by the recent structural characterization of $[\text{Rh}_2(\text{CO})_2(\mu\text{-Cl})(\text{DPM})_2][\text{BF}_4]$.⁵ In support of this mode of attack, the infrared spectra obtained during the slow stepwise addition of SO_2 to **1a** display no infrared bands assignable to bridging carbonyl species. On the basis of the analogous reaction of **1** with CO and the reaction of the *trans*-dichlorodicarbonyl species **8** with SO_2 (vide supra), both of which occur by terminal attack, we would have anticipated observing

species with bridging CO bands in the infrared spectra, if attack of **1** with SO_2 were also terminal. Furthermore, even at -50°C when the reaction is monitored by $^{31}\text{P}\{^1\text{H}\}$ NMR the only resonances observed are assignable to the symmetric species **1a** and **3a**. If attack were terminal, we would anticipate resonances assignable to an asymmetric species. We believe therefore that, on the basis of the above data, terminal attack of **1** by SO_2 can be ruled out, since no asymmetric species were detected. Furthermore we feel that it is unlikely that a facile rearrangement is operating since we can devise no simple rearrangement mechanism that would yield the symmetric bridged species **3a** from terminal attack. The reason for the different modes of attack of CO and SO_2 in complex **1** is at the present time not obvious.

Although we now understand much about the modes of attack and coordination of SO_2 in these binuclear systems as well as some of the subsequent chemistry of these SO_2 complexes, there are still some unanswered questions remaining, particularly relating to the differences in the chemistries of SO_2 and CO in these systems. It is anticipated that our continuing investigations in this area will help answer some of these unanswered questions and will extend our understanding of the chemistry of binuclear metal complexes.

Acknowledgment. The authors thank the National Science and Engineering Research Council of Canada and the University of Alberta for financial support, NSERC for a scholarship to S.K.D., Dr. A. R. Sanger for supplying the crystals of complex **4**, and Professor A. L. Balch for communication of his results prior to publication.

Registry No. **1a**, 67202-35-1; **1b**, 71647-00-2; **2b**, 71647-01-3; **3a**, 68080-76-2; **3b**, 71646-99-6; **4**, 69063-81-6; **6**, 22427-58-3; **8**, 22427-58-3; $[\text{RhCl}(\text{COD})]_2$, 12092-47-6.

Supplementary Material Available: Table IX, showing the idealized hydrogen parameters and a listing of the observed and calculated structure amplitudes (25 pages). Ordering information is given on any current masthead page.

(34) Cowie, M.; Dwight, S. K., to be submitted for publication.

Contribution from the Theoretical Division, Los Alamos Scientific Laboratory, Los Alamos, New Mexico 87545, and the Department of Chemistry, Harvard University, Cambridge, Massachusetts 02138

Stereochemical Rigidity and Isomerization in B_4H_4 and B_4F_4 . A Theoretical Study

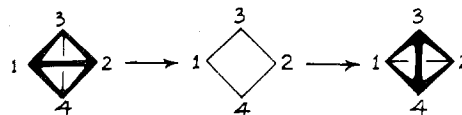
DANIEL A. KLEIER,*¹ JOSEF BICERANO, and WILLIAM N. LIPSCOMB

Received August 27, 1979

The degenerate rearrangement of both tetrahedral B_4H_4 and B_4F_4 along a least-motion pathway passes through a square-planar midpoint structure. This rearrangement is accompanied by an orbital crossing of the HOMO-LUMO type which is responsible for the imposition of a sizable barrier to the process. Both approximate and ab initio calculations including correlation were performed to characterize the pathway for these rearrangements. For B_4H_4 a barrier of approximately 85 kcal/mol is calculated while a smaller barrier is predicted for B_4F_4 . For both molecules the square midpoint structure may be a stable intermediate along the reaction pathway.

As part of a continuing study of rearrangements in closo boron hydrides,²⁻⁴ we report here on the nature of the stereochemical rigidity in B_4X_4 ($\text{X} = \text{H}, \text{F}$). The degenerate rearrangement of B_4X_4 provides the ultimate example of a diamond-square-diamond (dsd) transformation⁵ in a small

Scheme I



system (Scheme I). Previous theoretical studies have not considered the nature of the square midpoint structure nor the nature of the electronic reorganization required for the dsd transformation in B_4X_4 .

(1) Camille and Henry Dreyfus Teacher-Scholar Grantee, 1979-1984. Address correspondence to Thompson Chemical Laboratory, Williams College, Williamstown, MA 01267.

(2) D. A. Kleier, D. A. Dixon, and W. N. Lipscomb, *Inorg. Chem.*, **17**, 166 (1978).

(3) D. A. Kleier and W. N. Lipscomb, *Inorg. Chem.*, **18**, 1312 (1979).

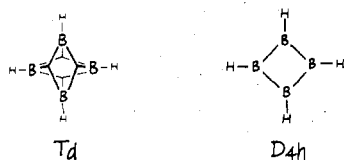
(4) I. M. Pepperburg, T. A. Halgren, and W. N. Lipscomb, *J. Am. Chem. Soc.*, **97**, 1284 (1975).

(5) W. N. Lipscomb, *Science*, **153**, 373 (1966).

Table I. Optimized Geometries and Energies of B_4H_4 and B_4F_4

A. Bond Lengths (Å)							
molecule	struct	bond	length	molecule	struct	bond	length
B_4H_4	T_d	BB	1.640	B_4F_4	T_d	BB	1.683
		BH	1.142			BF	1.308
	D_{4h}	BB	1.699		D_{4h}	BB	1.720
		BH	1.145			BF	1.344
B. Energies (au)							
molecule	struct	$E(\text{PRDDO})$		$E(\text{ab initio})$		$E(\text{CI})$	
B_4H_4	T_d	-100.853	} 25.1 ^a	-99.689 ^b	} 38.8 ^a	-99.890 ^d	} 75.2 ^a
	D_{4h}	-100.813		-99.627 ^b		-99.770 ^d	
B_4F_4	T_d	-494.692	} -17.6 ^a	-496.562 ^c	} 10.0 ^a	-494.734 ^e	} 0.6 ^a
	D_{4h}	-494.720		-496.546 ^c		-494.733 ^e	

^a Differences are expressed in units of kcal/mol. ^b HF results with STO-3G basis (W. J. Hehre, R. F. Stewart, and J. A. Pople, *J. Chem. Phys.*, **51**, 2657 (1969)). ^c HF results with a double- ζ basis (T. H. Dunning and P. J. Hay in "Methods of Electronic Structure", H. F. Schaeffer III, Ed., Plenum, Press, New York, 1977, p 1). ^d All single and double excitations within the valence space from configurations I and II. ^e Limited CI (18 single and 126 double excitations from HF wave function) using PRDDO integral list.

Figure 1. Localized molecular orbital structures for B_4H_4 .

The localized molecular orbital (LMO) structures⁶ for B_4H_4 are presented in Figure 1. The framework LMO's for B_4F_4 ⁹ are qualitatively identical with those for B_4H_4 . Although the framework orbitals within each structure are equivalent, they span different representations of the D_{2d} subgroup that is common to both the tetrahedral (T_d) and square-planar (D_{4h}) structures. For the T_d structure the framework LMO's span an $a_1 + e + b_2$ representation of D_{2d} while for the D_{4h} structure they span an $a_1 + e + b_1$ representation. Thus, an orbital crossing must occur along the least motion path connecting these two structures. The situation in terms of the symmetry orbitals is depicted in Figure 2. The HOMO of the T_d structure is a triply degenerate t_2 orbital, and only the b_2 component is depicted. It is clearly a bonding orbital for the B_1, B_2 and B_3, B_4 pairs of boron atoms. As the tetrahedron is flattened in the sense of Scheme I, the degeneracy is lifted and the b_2 orbital energy rises ultimately correlating with the LUMO of the D_{4h} structure. The HOMO of the D_{4h} structure has b_1 symmetry under the D_{2d} subgroup and is a bonding orbital for adjacent borons in the square but an antibonding orbital for catty-cornered borons. Thus, its energy rises as the catty-cornered borons approach one another during the D_{4h} to T_d transformation ultimately correlating with a component of the e-type LUMO of the T_d structure.

For a quantitative characterization of the potential energy surface for the dsd transformation of B_4H_4 , the limiting geometries were first completely optimized at the Hartree-Fock (HF) level by using the PRDDO approximation.¹¹ The optimized geometries and energies are given in Table I. Due

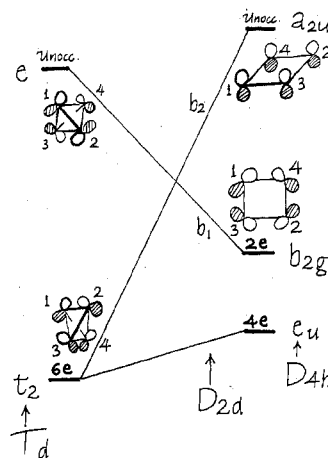


Figure 2. MO correlation diagram for the T_d to D_{4h} transformation of B_4H_4 . For B_4H_4 the b_{2g} and e_u orbitals of the D_{4h} structure are interchanged. Symmetry designations on tie lines are for the D_{2d} subgroup of both T_d and D_{4h} . Only the contributions from the boron atoms are shown.

Table II. Energy of B_4H_4 along the Linear Synchronous Transit Pathway

R	$E(\text{GVB}),^a$ au	GVB coeff ^a		$E(\text{CI}),^b$ au	CI coeff ^c	
		I	II		I	II
0.0 (T_d)	-99.690	0.999	-0.027	-99.890	0.941	
0.2	-99.678	0.999	-0.029	-99.882	0.938	
0.4	-99.640	0.998	-0.056	-99.850	0.932	
0.6	-99.588	0.958	-0.288	-99.803	0.926	
0.7	-99.591	0.192	-0.981	-99.774	0.913	-0.103
0.8	-99.605	0.104	-0.995	-99.755	0.392	-0.867
0.9	-99.617	0.075	-0.997	-99.763	0.086	-0.953
1.0 (D_{4h})	-99.627	0.060	-0.998	-99.770		-0.956

^a The GVB coefficients are those for configurations I and II in the natural orbital representation of the GVB wave function.¹² These calculations were carried out with an STO-3G basis. ^b Includes all single and double excitations within valence space from configurations I and II. ^c CI coefficients were not printed if the estimated contribution to the energy lowering was less than 10^{-4} au.

to the orbital crossing a minimum of two configurations is required to describe the wave function along the transformation pathway. Thus, two-configuration SCF calculations were performed by using the GVB procedure¹² for several points

(6) These structures were obtained by using the Boys criterion⁷ as described in ref 8.

(7) (a) S. F. Boys in "Quantum Theory of Atoms, Molecules, and the Solid State", P. O. Lowdin, Ed., Academic Press, New York, 1966, p 253; (b) J. M. Foster and S. F. Boys, *Rev. Mod. Phys.*, **32**, 300 (1960).

(8) D. A. Kleier, T. A. Halgren, J. H. Hall, Jr., and W. N. Lipscomb, *J. Chem. Phys.*, **61**, 3905 (1974).

(9) (a) J. H. Hall, T. A. Halgren, D. A. Kleier, and W. N. Lipscomb, *Inorg. Chem.*, **13**, 2520 (1974); (b) M. F. Guest and I. H. Hillier, *J. Chem. Soc., Faraday Trans. 2*, **70**, 398 (1974).

(10) The b_{2g} (b_1) orbital depicted in Figure 2 is the HOMO for B_4F_4 . For B_4H_4 (D_{4h}) the b_{2g} and e_u orbitals are nearly degenerate with the b_{2g} lying slightly below the e_u orbital.

(11) (a) T. A. Halgren and W. N. Lipscomb, *J. Chem. Phys.*, **58**, 1569 (1973); (b) T. A. Halgren, D. A. Kleier, J. H. Hall, Jr., L. D. Brown, and W. N. Lipscomb, *J. Am. Chem. Soc.*, **100**, 6595 (1978).

(12) W. J. Hunt, P. J. Hay, and W. A. Goddard, *J. Chem. Phys.*, **57**, 738 (1972).

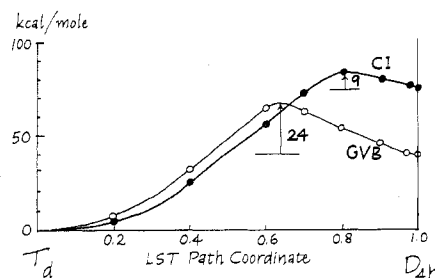


Figure 3. Total energy of two-configuration SCF (designated GVB) and CI wave functions for B_4H_4 along the linear synchronous transit pathway. Energies are from Table II.

along a linear synchronous transit (LST) pathway¹³ connecting the T_d and D_{4h} limiting structures. The configurations included are

$$\dots t_2^6 = \dots e^4 b_2^2 \quad (\text{I})$$

$$\dots e_u^4 b_{2g}^2 = \dots e^4 b_1^2 \quad (\text{II})$$

where the symmetry designations on the left are those for the T_d and D_{4h} groups, respectively, and those on the right are those for the D_{2d} subgroup common to both structures.

The results for the two-configuration SCF calculations are given in Table II and plotted in Figure 3. A rather pronounced barrier of about 67 kcal/mol occurs at a path coordinate¹³ of ~ 0.62 and corresponds to a change in the description of the wave function from predominantly configuration I to configuration II. The electronic structure at this point has an unusual biradical character. One radical is localized along the 1-3 and 2-4 edges of the partially flattened tetrahedron while the other is localized along the 1-4 and 2-3 edges (see Scheme I).

CI calculations were performed for points along the LST path by including all single and double excitations from the occupied valence orbitals of configurations I and II. Inclusion of this additional correlation delays the barrier to a path coordinate of ~ 0.80 , raises the barrier for the $T_d \rightarrow D_{4h}$ transformation to 85 kcal/mol, and, due to the extra correlation stabilization enjoyed by the more compact T_d structure, raises the overall energy change for the transformation from an HF value of 39.0 to 75.0 kcal/mol (Table I). Of course it is possible that orthogonal optimization of the "transition state" will remove the barrier for the $T_d \rightarrow D_{4h}$ transformation, but the existence of such a barrier seems consistent with the observed orbital crossing.

Somewhat surprisingly when the T_d and D_{4h} structures of B_4F_4 were optimized at the PRDDO level (Table I), the D_{4h} structure was found to be most stable. Therefore, we performed limited CI calculations at the PRDDO level of approximation as well as double- ζ HF calculations of an ab initio nature on both of the limiting forms. As Table I reveals, the more compact T_d structure was favored by both of these more sophisticated calculations though the preference for the T_d structure is still significantly less strong than was the case for B_4H_4 . The reason that the planar D_{4h} structure of B_4F_4 is more stable than that of B_4H_4 relative to the corresponding T_d structures may be ascribed in part to the enhanced degree of

Table III. Population Analyses^a of PRDDO Wave Functions

struct	atomic charge	degree of bonding	total valency			
A. B_4H_4						
T_d	B_1	-0.001	B_1-B_2	0.879	B	14.546
	H_1	0.001	B_1-H_1	0.986	H	3.999
D_{4h}	B_1	0.039	B_1-B_2	0.008	B	11.990
	H_1	-0.039	B_1-B_3	0.996	H	3.995
			B_1-H_1	0.988		
B. B_4F_4						
T_d	B_1	0.075	B_1-B_2	0.760	B	14.678
	F_1	-0.075	B_1-F_1	1.218	F	5.661
D_{4h}	B_1	0.074	B_1-B_2	0.021		
	F_1	-0.074	B_1-B_3	0.940	B	13.208
			B_1-F_1	1.331	F	5.635

^a Reference 14.

bonding¹⁴ enjoyed by the BF bonds in the planar structure of B_4F_4 (Table IIIB). No such enhancement is observed for B_4H_4 . Furthermore, although the valency¹⁴ within the boron framework of both B_4F_4 and B_4H_4 decreases in the $T_d \rightarrow D_{4h}$ transformation, the decrease is considerably less in both an absolute and a relative sense for B_4F_4 . Of course, a detailed population analysis of our double- ζ results for B_4F_4 may have diminished the differences between B_4F_4 and B_4H_4 in this respect, but qualitatively we expect the same trends to hold.

Two-configuration SCF calculations performed at the PRDDO level for B_4F_4 at various points along the $T_d \rightarrow D_{4h}$ pathway reveal a substantial barrier for passage in both directions. The maximum on the LST path relative to the T_d structure is about 44 kcal/mol and about 61 kcal/mol relative to the D_{4h} structure. Inclusion of correlation effects is expected to substantially increase the former figure.

B_4Cl_4 , the only known borane possessing the B_4X_4 composition, has a tetrahedral structure in the crystalline phase.¹⁵ This is consistent with our double- ζ results for B_4F_4 . However, due to the relatively small energy differences calculated for the planar and tetrahedral forms of B_4F_4 and the likelihood of a substantial energy barrier separating them, we are led to propose that B_4F_4 (once synthesized) and B_4Cl_4 will exist under proper conditions as either the tetrahedral or the planar isomer or a mixture of both.

In contrast to B_4H_4 and B_4F_4 with their high barriers to degenerate rearrangement stand the highly fluxional closo boron hydrides such as $B_8H_8^{2-3}$ and $B_{11}H_{11}^{2-2}$.² In neither of the latter cases is a HOMO-LUMO crossing required for degenerate rearrangements. These results prompt us to hypothesize that degenerate rearrangements of rigid closo boron hydrides involve HOMO-LUMO-like crossings or intended crossings, while rearrangements of fluxional members of this homologous series suffer no such requirement.

Acknowledgment. We are grateful to P. J. Hay for helpful comments. We thank the National Science Foundation (Grant CHE 7719899) for partial support of the research. Part of the research was carried out under the auspices of the U.S. Department of Energy. D.A.K. acknowledges a sabbatical leave from Williams College.

Registry No. B_4H_4 , 27174-99-8; B_4F_4 , 49567-49-9.

(14) D. R. Armstrong, P. G. Perkins, and J. P. Stewart, *J. Chem. Soc., Dalton Trans.*, 838 (1973).

(15) (a) G. Urry, T. Wortik, and H. Schlesinger, *J. Am. Chem. Soc.*, **74**, 5809 (1952); (b) M. A. Toji and W. N. Lipscomb, *J. Chem. Phys.*, **21**, 172 (1953); (c) *Acta Crystallogr.*, **6**, 547 (1953).

(13) T. A. Halgren and W. N. Lipscomb, *Chem. Phys. Lett.*, **49**, 225 (1977).